

An approximate solution for the Couette–Poiseuille flow of the Giesekus model between parallel plates

Ahmadreza Raisi · Mahmoud Mirzazadeh ·
Arefeh Sadat Dehnavi · Fariborz Rashidi

Received: 11 January 2007 / Accepted: 10 May 2007 / Published online: 18 June 2007
© Springer-Verlag 2007

Abstract An approximate analytical solution is derived for the Couette–Poiseuille flow of a nonlinear viscoelastic fluid obeying the Giesekus constitutive equation between parallel plates for the case where the upper plate moves at constant velocity, and the lower one is at rest. Validity of this approximation is examined by comparison to the exact solution during a parametric study. The influence of Deborah number (De) and Giesekus model parameter (α) on the velocity profile, normal stress, and friction factor are investigated. Results show strong effects of viscoelastic parameters on velocity profile and normal stress. In addition, five velocity profile types were obtained for different values of α , De , and the dimensionless pressure gradient (G).

Keywords Giesekus constitutive equation ·
Couette–Poiseuille flow · Viscoelastic fluid ·
Parallel plates

Introduction

Through the years, many authors have tried to analyze the flow of different classes of materials in ducts and channels using various constitutive equations such as inelastic and linear/nonlinear viscoelastic models. An extensive literature review on this subject can be found in Pinho and Oliveira (2000), Alves et al. (2001), Escudier et al. (2002), and Oliveira (2002).

The flow of non-Newtonian fluids between parallel plates is also a problem of considerable practical interest. Because of their simplicity and originality, parallel plates are often used to simulate the actual flow domain conditions in single screw extruders. Because a narrow gap exists between the barrel and the screw of the extruder, the assumption of fluid flowing between parallel plates leads to meaningful and accurate results. Tadmor and Gogos (1979) published an extensive compilation of the available information and mathematical explanation for single screw extrusion.

Giesekus (1982) has developed a three-parameter model using molecular ideas that is nonlinear in the stresses. This model has gained prominence because it describes the power-law regions for viscosity and normal-stress coefficients; it also gives a reasonable description of the elongational viscosity and the complex viscosity. This model incorporates shear-thinning shear viscosity, nonvanishing normal-stress differences, extensional viscosity with finite asymptotic value, and nonexponential stress relaxation and start-up curves. Thus, it reproduces many characteristics of the rheology of polymer solutions as well as other liquids.

The Giesekus model is employed increasingly to predict the flow and heat transfer of viscoelastic fluids. Yoo and Choi (1989) studied the Giesekus model (without retardation time) in plane Couette–Poiseuille flows and obtained analytic solutions. Later, Schleiniger and Weinacht (1991) studied the steady Poiseuille flow in channels and pipes for the same model (with and without solvent contribution). They showed the possibility of the infinite number of weak solutions for the boundary value problem, in addition to the classical ones of Yoo and Choi (1989). They also showed that only the classical solutions are physically relevant solutions. Mostafaiyan et al. (2004) used the Giesekus model and obtained solution for the axial annular flow of a

A. Raisi · M. Mirzazadeh · A. S. Dehnavi · F. Rashidi (✉)
Department of Chemical Engineering,
Amirkabir University of Technology (Tehran Polytechnic),
Hafez Ave.,
P.O. Box 15875-4413, Tehran, Iran
e-mail: Rashidi@aut.ac.ir

viscoelastic flow. They proposed an approximation to the radial normal stress estimation that results in an analytic expression for the velocity and pressure profiles.

The solution of viscous dynamic pressurization for a Giesekus model fluid moving between parallel plates with one of the plates in motion has not yet been reported. The objective of the present paper is to solve analytically the momentum governing equation for such a system. The analytical solution derived in this investigation can be used as a benchmark to validate numerical results and is more convenient to describe some specific fluid behaviors.

Problem statement

A schematic diagram of a problem under consideration is shown in Fig. 1. The geometry consists of two parallel plates that are infinite in the x direction and wide enough in the z direction to have negligible side effects.

The problem under consideration is steady, laminar, and fully developed. Therefore, the axial velocity (u) is the only function of y , and the imposed pressure gradient is constant. The no-slip condition exists at the walls, and the gravitational forces for the flow domain are negligible. Under these conditions, equations of continuity and momentum (neglecting gravity) are given as follows:

$$\nabla \cdot u = 0 \quad (1)$$

$$\rho \frac{Du}{Dt} + \nabla P = \nabla \cdot \tau \quad (2)$$

The Giesekus (1982) model, which is used as the rheological model, is as follows:

$$\tau + \frac{\alpha\lambda}{\eta} (\tau \cdot \tau) + \lambda \frac{\partial \tau}{\partial t} = 2\eta D \quad (3)$$

where:

$$D = \frac{1}{2} (\nabla u + (\nabla u)^T) \quad (4)$$

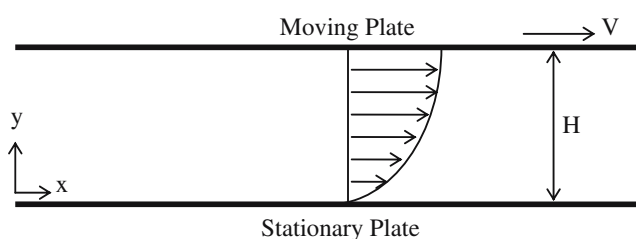


Fig. 1 Schematic diagram of flow domain

$$\frac{\partial \tau}{\partial t} = \frac{D\tau}{Dt} - (\tau \cdot \nabla u + (\nabla u)^T \cdot \tau) \quad (5)$$

$$\frac{D\tau}{Dt} = \frac{\partial \tau}{\partial t} + (u \cdot \nabla) \tau \quad (6)$$

η and λ are the model parameters representing zero-shear viscosity and zero-shear relaxation time, respectively (Giesekus 1983). The parameter α in Eq. 3 is a model parameter, and the term containing α has been attributed to anisotropic Brownian motion or anisotropic hydrodynamic drag on the constituent polymer molecules (Bird et al. 1987), and it is required that $0 \leq \alpha < 1$ as discussed by Giesekus (1982). Setting $\alpha=0$ reduces the model to the upper convected Maxwell.

The flow is assumed to be laminar, steady state, isothermal, and incompressible. Under these conditions, Eq. 2 reduces to:

$$\frac{dP}{dx} = \frac{d\tau_{yx}}{dy} \quad (7)$$

Introducing the following dimensionless quantities:

$$y^* = \frac{y}{H}; x^* = \frac{x}{H}; u^* = \frac{u}{V}; \tau^* = \frac{\tau H}{\eta V}; \text{De} = \frac{\lambda V}{H}; G = \frac{H^2}{\eta V} \left(\frac{dP}{dx} \right) \quad (8)$$

where the dimensionless group De is the Deborah number, which is related to the level of elasticity of the fluid, and G is a dimensionless group for pressure drop. For Newtonian fluids, the ratio of the pure drag flow rate to the pure pressure flow rate is equal to $6/G$. The pure drag flow rate corresponds to the situation when the axial pressure gradient is zero ($\frac{dP}{dx} = 0$), while the pure pressure flow rate applies for stationary parallel plates (Tadmor and Gogos 1979).

The dimensionless form of the equations of motion and the constitutive equation are as follows:

$$\frac{d\tau_{yx}^*}{dy^*} = G \quad (9)$$

$$\tau_{yy}^* + \alpha \text{De} (\tau_{yy}^{*2} + \tau_{yx}^{*2}) = 0 \quad (10)$$

$$\tau_{xx}^* + \alpha \text{De} (\tau_{xx}^{*2} + \tau_{yx}^{*2}) - 2\text{De} \tau_{yx}^* \dot{\gamma}_{yx}^* = 0 \quad (11)$$

$$\tau_{yx}^* + \alpha \text{De} \tau_{yx}^* (\tau_{xx}^* + \tau_{yy}^*) - \text{De} \tau_{yx}^* \dot{\gamma}_{yx}^* = \dot{\gamma}_{yx}^* \quad (12)$$

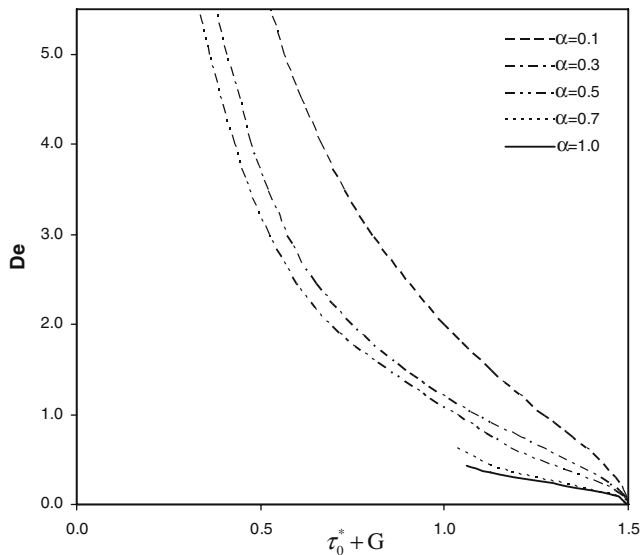


Fig. 2 The Deborah number vs the dimensionless shear stress for different values of parameter α

The dimensionless shear stress (τ_{yx}^*) can be obtained by integrating Eq. 9:

$$\tau_{yx}^* = \tau_0^* + Gy^* \tag{13}$$

τ_{yx}^* is a linear function of y^* and, as a specific case, is constant in the absence of pressure gradient; τ_0^* is the

dimensionless shear stress at the stationary plate. Eq. 10 is the second order with respect to τ_{yx}^* , hence:

$$\tau_{yy}^* = \frac{-1 \mp \sqrt{1 - 4\alpha^2 De^2 \tau_{yx}^{*2}}}{2\alpha De} \tag{14}$$

The classical positive and negative solutions of Eq. 14 have been discussed by Schleiniger and Weinacht (1991) using linear stability analysis and the requirements arising from configuration tensor. They concluded that, for the case of no-solvent viscosity, there is only one physically stable solution, which is the positive solution with the following restrictions:

$$|\tau_{yx}^*| < \frac{1}{De} \sqrt{\frac{1}{\alpha} - 1}; \quad 0 < \alpha \leq 0.5 \tag{15}$$

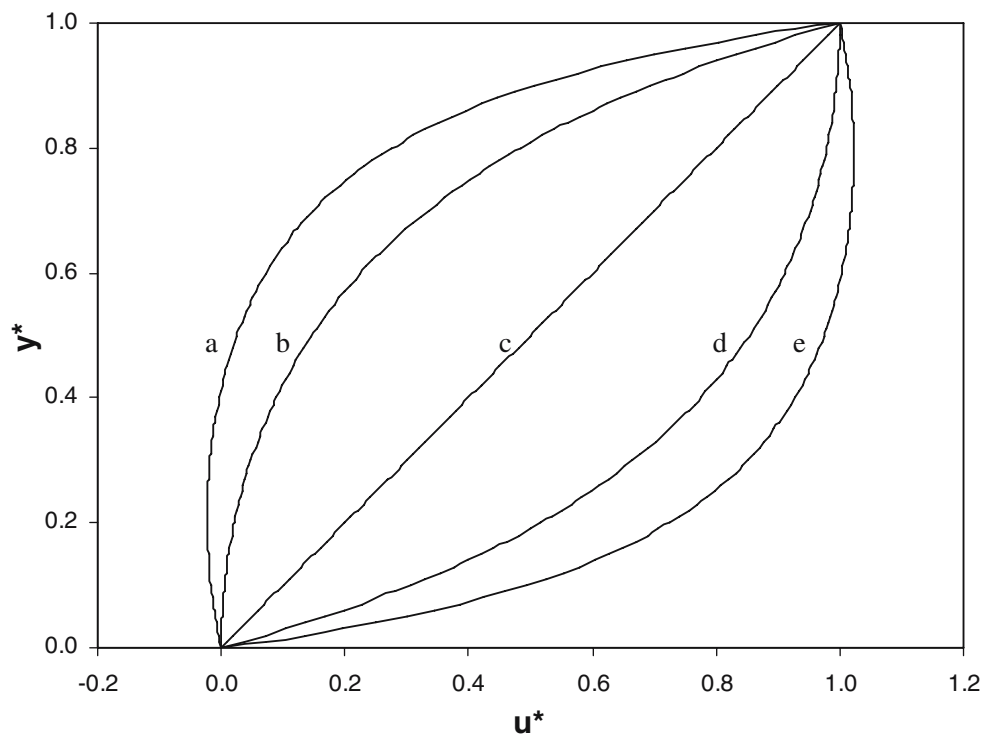
$$|\tau_{yx}^*| < \frac{1}{2\alpha De}; \quad 0.5 < \alpha \leq 1 \tag{16}$$

Yoo and Choi (1989) used a different approach for stability analysis. They concluded that, for the case of no-solvent solution and to obtain a real solution for the normal stress (Eq. 14), it is necessary to apply the following condition:

$$1 - 4\alpha^2 De^2 \tau_{yx}^{*2} \geq 0 \tag{17}$$

In addition to this, the first normal stress difference ($\tau_{xx} - \tau_{yy}$) must be positive from thermodynamic considerations.

Fig. 3 Five types of velocity profile for the Couette–Poiseuille flow, (a): $\alpha=0.3$, $De=2$, $G=1$; (b): $\alpha=0.1$, $De=2$, $G=1$; (c): $\alpha=0.1$, $De=2$, $G=0$; (d): $\alpha=0.1$, $De=2$, $G=-1$; (e): $\alpha=0.3$, $De=2$, $G=-1$



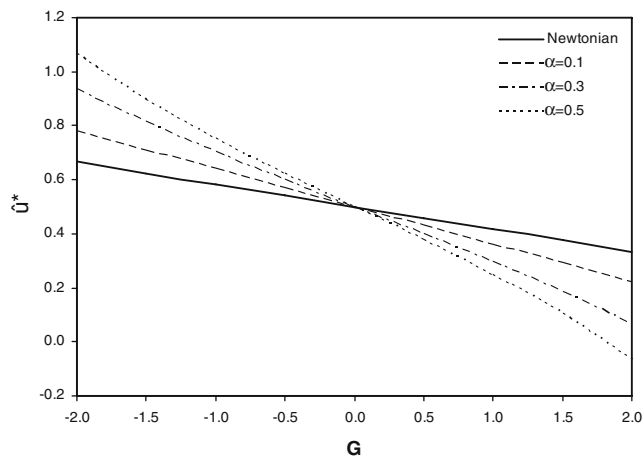


Fig. 4 The effect of the dimensionless pressure gradient on the average velocity for different viscoelastic parameters (linear stress coefficient, $De=1$)

Applying these conditions will result in the same equations as Eqs. 15 and 16.

From Eq. 12, τ_{xx}^* can be expressed as follows:

$$\tau_{xx}^* = \frac{(1 + De\tau_{yy}^*) \dot{\gamma}_{yx}^*}{\alpha De \tau_{yx}^*} - \frac{1 + \alpha De \tau_{yy}^*}{\alpha De} \quad (18)$$

By substituting Eq. 18 into Eq. 11 and using Eq. 10, $\dot{\gamma}_{yx}^*$ is obtained as:

$$\dot{\gamma}_{yx}^* = \frac{1 + (2\alpha - 1)De\tau_{yy}^*}{(1 + De\tau_{yy}^*)^2} \tau_{yx}^* \quad (19)$$

where $\dot{\gamma}_{yx}^* = \frac{du_x^*}{dy^*}$ and the boundary conditions are:

$$y^* = 0 \quad ; \quad u_x^* = 0 \quad (20)$$

$$y^* = 1 \quad ; \quad u_x^* = 1 \quad (21)$$

The velocity profile can be obtained from:

$$u_x^* = \int \dot{\gamma}_{yx}^* dy^* + C \quad (22)$$

Eq. 22 is integrated using the Gaussian quadrature method to obtain the velocity profile, and τ_o^* is found by applying boundary conditions (Eqs. 20 and 21) and using an iteration scheme.

The term $\sqrt{1 - 4\alpha^2 De^2 \tau_{yx}^{*2}}$ in Eq. 14 can be expressed in power series using the binomial expansion, resulting in the following expression:

$$\tau_{yy}^* = -\alpha De \tau_{yx}^{*2} (1 + \alpha^2 De^2 \tau_{yx}^{*2} + \dots) \approx -\alpha De \tau_{yx}^{*2} \quad (23)$$

Note that, in the approximation, all terms of higher order have been neglected compared to the leading term. This is valid for small values of $4\alpha^2 De^2 \tau_{yx}^{*2}$.

By substituting Eq. 23 into Eq. 19:

$$\dot{\gamma}_{yx}^* = \frac{du_x^*}{dy^*} = \frac{1 - \alpha(2\alpha - 1)De^2 \tau_{yx}^{*2}}{(1 - \alpha De^2 \tau_{yx}^{*2})^2} \tau_{yx}^* \quad (24)$$

Substituting τ_{yx}^* from Eq. 13 in the above equation, it is possible to integrate Eq. 22 to obtain the following analytical expression for the velocity profile:

$$u_x^* = -\frac{1}{2\alpha G De^2} \left[\frac{2(\alpha-1)}{1 - \alpha De^2 (\tau_o^* + Gy^*)^2} + (2\alpha - 1) \ln(1 - \alpha De^2 (\tau_o^* + Gy^*)^2) \right] + C \quad (25)$$

By introducing the boundary conditions from Eqs. 20 and 21 into Eq. 25, the following relation can be derived:

$$\frac{2\alpha - 1}{2\alpha De^2 G} \ln \left(\frac{1 - \alpha De^2 \tau_o^{*2}}{1 - \alpha De^2 (\tau_o^* + G)^2} \right) - \frac{(\alpha - 1)(G + 2\tau_o^*)}{(1 - \alpha De^2 \tau_o^{*2})(1 - \alpha De^2 (\tau_o^* + G)^2)} - 1 = 0 \quad (26)$$

Eq. 26 is strongly nonlinear but can be solved numerically for the dimensionless shear stress τ_o^* at the stationary plate. The Newton–Raphson method is used for the solution of Eq. 26, where the Newtonian value of τ_o^* is used as an initial guess. Once τ_o^* is known, determination of constant C in Eq. 25 is straightforward: C is obtained from Eq. 25 and by applying the first boundary condition (Eq. 20).

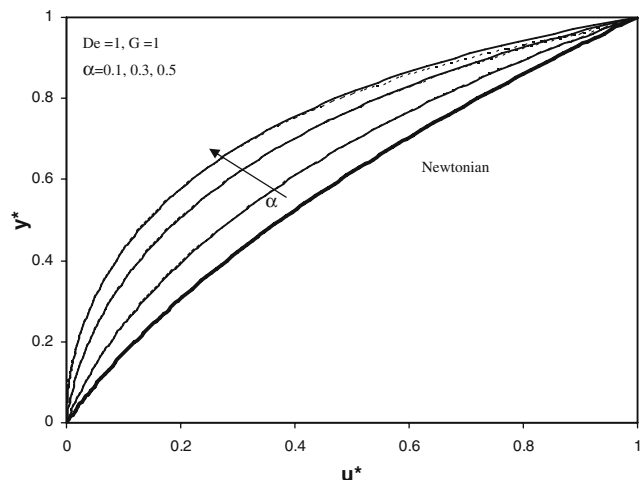


Fig. 5 Effect of α on velocity profile for $De=1$ and $G=1$. The solid lines and dashed lines represent the approximate and exact solution, respectively

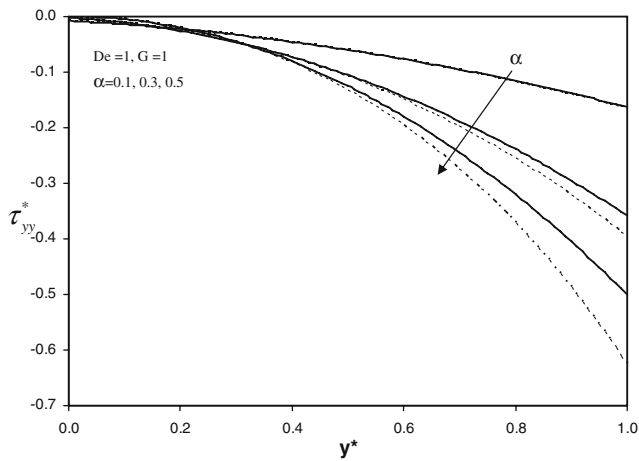


Fig. 6 Effect of α on normal stress (τ_{yy}^*) for $De=1$ and $G=1$. The *solid lines* and *dashed lines* represent the approximate and exact solution, respectively

Results and discussion

In the following, a parametric study of the obtained approximate solution is performed using different values for α , De , and G . As discussed by Bird et al. (1987), it is required that $0 < \alpha \leq 0.5$ to obtain realistic properties. Figure 2 shows that for $0.5 < \alpha \leq 1$, there are limiting values for De based on Eq. 16. As can be seen from this figure, by increasing the value of α , the range of acceptable Deborah numbers becomes narrower. A similar conclusion was achieved by Yoo and Choi (1989). Therefore, in this work, the parametric study was performed only for the range $0 < \alpha \leq 0.5$.

The shape of the velocity profile is strongly influenced by the competition between drag and pressure flows as well as by the De and model parameters. Different types of

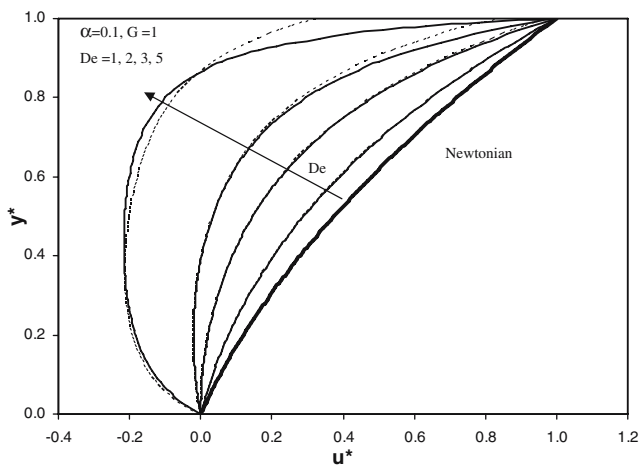


Fig. 7 Effect of De on velocity profile for $\alpha=0.1$ and $G=1$. The *solid lines* and *dashed lines* represent the approximate and exact solution, respectively

dimensionless velocity distributions that are obtained for various values of α , De , and G for Couette–Poiseuille flow are illustrated in Fig. 3. When G is positive, the upstream pressure is lower than the downstream pressure, which may yield back flow through the channel (Fig. 3a,b). In this case, the direction of the pressure flow is negative, while the drag flow acts in the positive direction. When G is equal to zero, there is no effect of pressure flow, and dimensionless velocity profile is linear, as shown in Fig. 3c. For negative G values, the drag and pressure flows are in the same direction, and positive values for \hat{u}^* are obtained (Fig. 3d,e).

Effect of dimensionless pressure gradient

The dimensionless pressure gradient is usually unknown, but it is related to the cross-sectional average velocity through the following equation:

$$\hat{u}^* = \int_0^1 u_x^* dy^* \tag{27}$$

Substitution of Eq. 25 results in:

$$\hat{u}^* = \left(\frac{1-2\alpha}{2\alpha De^2 G}\right) 1n\left(1 - \frac{1}{3}\alpha De^2 G - \alpha De^2 G \tau_0^* - \alpha De^2 \tau_0^{*2}\right) + \left(\frac{1-\alpha}{\alpha^{1.5} De^4 G^2}\right) \left(\arctan h\left[\alpha^{0.5} De(G + \tau_0^*)\right] - \arctan h\left[\alpha^{0.5} De \tau_0^*\right]\right) + C \tag{28}$$

The values of G are calculated numerically using different values of the flow rate, model parameter, and De . Based on the sign of the pressure gradient, G may be positive or negative. Figure 4 represents the variation of the dimensionless average velocity (\hat{u}^*) as a function of the

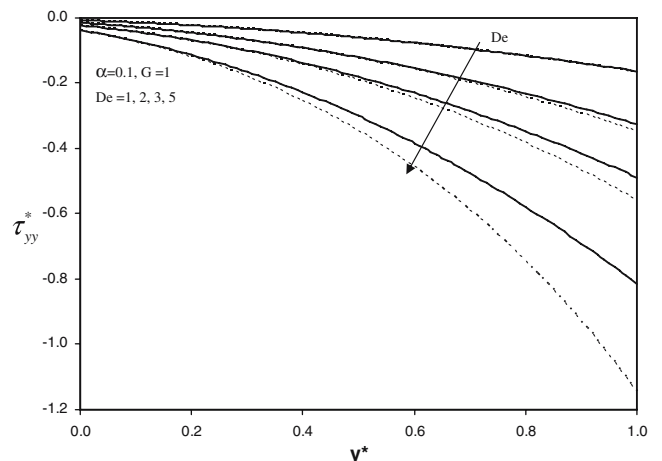


Fig. 8 Effect of De on normal stress (τ_{yy}^*) for $\alpha=0.1$ and $G=1$. The *solid lines* and *dashed lines* represent the approximate and exact solution, respectively

dimensionless pressure gradient (G) for different values of α and De . For positive values of dimensionless pressure gradient, the deviation of average velocity with respect to the Newtonian value increases with the viscoelastic dimensionless group. This deviation increases as the dimensionless pressure gradient is decreased.

For negative values of G , the reverse is true, but the deviations are much higher. An average velocity equal to 0.5 corresponds to a dimensionless pressure drop of zero, which corresponds to a pure drag flow.

Effect of Giesekus model parameter

The effect of α on the dimensionless velocity profile at $De=1$ and $G=1$ for different values of α is illustrated in Fig. 5. In this figure, solid lines represent the results for approximate solution, while dashed lines represent the results for exact solution. The arrow indicates the increasing direction of the parameter under study. As can be seen from this figure, the velocity gradient increases as the α increases, i.e., as the shear-thinning behavior of the fluid increases.

Figure 6 shows the effect of α on normal stress. Again, the solid lines and dashed lines represent the approximate and exact solutions, respectively. As shown in this figure, the absolute value of dimensionless normal stresses increase as the value of α increases (i.e., as the fluid elasticity increases).

Effect of Deborah number

The effect of De on the dimensionless velocity profile and normal stress at $\alpha=0.1$ and $G=1$ for different values of De are presented in Figs. 7 and 8, respectively. The solid lines and dashed lines represent the approximate and exact solutions, respectively. As illustrated in these figures, the effect of De is approximately the same as the effect of α , but in this case, the deviation from Newtonian velocity profile is larger. Figure 7 shows that, for small values of α , increasing De causes significant deviation from Newtonian values.

In addition, Figs. 5, 6, 7, and 8 reveal that, at small values of De and α , the approximate solution follows the solution obtained from the numerical integration of the exact equations very closely. However, the difference increases as α and De increase. Because by increasing the values of α and De , the term $4\alpha^2 De^2 \tau_{yx}^{*2}$ in Eq. 14 increases, and consequently, the truncation error increases.

Conclusions

An approximate analytical solution for steady, laminar, incompressible flow of the Giesekus model fluid, through parallel plates while lower plate is stationary, but the upper plate is moving at a constant velocity, is obtained. Effects of material parameters, flow conditions, and geometry on the velocity profile and normal stress are studied. Results for the linear stress coefficient emphasize the appreciable influence that α and De have on the flow behavior. For negative values of G , an increase in α or De leads to an increase in the velocity profile and normal stress for combined drag and pressure flows, whereas the reverse behavior occurs for positive values of G . Comparative study of the approximate and exact solutions show that approximate solution has good accuracy for low α and De .

Finally, a particular application of this work maybe achieved by implementing it to estimate the flow behavior of viscoelastic fluid for single screw extruders.

References

- Alves MA, Pinho FT, Oliveira PJ (2001) Study of steady pipe and channel flows of a single-mode Phan–Thien–Tanner fluid. *J Non-Newtonian Fluid Mech* 101:55–76
- Bird RB, Armstrong RC, Hassager O (1987) Dynamics of polymeric liquids, fluid dynamics, vol. 1, 2nd edn, Wiley, New York
- Escudier MP, Oliveira PJ, Pinho FT (2002) Fully developed laminar flow of purely viscous non-Newtonian liquids through annuli, including the effects of eccentricity and inner-cylinder rotation. *Int J Heat Fluid Flow* 23:52–73
- Giesekus H (1982) A simple constitutive equation for polymer fluids based on the concept of deformation-dependent tensorial mobility. *J Non-Newtonian Fluid Mech* 11:69–109
- Giesekus H (1983) Stressing behavior in simple shear flow as predicted by a new constitutive model for polymer fluids. *J Non-Newtonian Fluid Mech* 12:367–374
- Mostafaiyan M, Khodabandehlou Kh, Sharif F (2004) Analysis of a viscoelastic fluid in an annulus using Giesekus model. *J Non-Newtonian Fluid Mech* 118:49–55
- Oliveira PJ (2002) An exact solution for tube and slit flow of FENE-P fluid. *Acta Mech* 158:157–167
- Pinho FT, Oliveira PJ (2000) Axial annular flow of a nonlinear viscoelastic fluid—an analytical solution. *J Non-Newtonian Fluid Mech* 93:325–337
- Schleiniger G, Weinacht R (1991) Steady Poiseuille flows for a Giesekus fluid. *J Non-Newtonian Fluid Mech* 40:79–102
- Tadmor Z, Gogos C (1979) Principles of polymer processing. Wiley, New York
- Yoo JY, Choi HCh (1989) On the steady simple shear flows of the one-mode Giesekus fluid. *Rheol Acta* 28:13–24